

On the Mean Free Path for Backscattering in $k_B T$ Layer of Bulk Nano-MOSFETs

Ming-Jer Chen, *Senior Member, IEEE*, Li-Fang Lu, and Chih-Yu Hsu, *Student Member, IEEE*

Abstract—We perform Monte Carlo particle simulations on a silicon conductor for the purposes of reexamining the channel backscattering in *bulk* nano-MOSFETs. The resulting mean free path λ_o for backscattering in a long and near-equilibrium conductor is constant, regardless of the potential profile. However, the *apparent* mean free path λ_1 in a local quasi-ballistic $k_B T$ layer depends on the curvature of the potential profile. In a linear potential profile, the λ_1 extracted in a wide range of the conductor length (15 to 100 nm) and lattice temperature (150 to 300 K) is found to fall below λ_o . The carrier heating as the origin of reduced mean free path is inferred from the simulated carrier velocity distribution near the injection point. Strikingly, the mean free paths in a parabolic potential profile remain consistent: $\lambda_1 = \lambda_o$. This indicates the absence or weakening of the carrier heating in the layer of interest, valid only for the parabolic potential barrier.

Index Terms—Backscattering, MOSFET, nanoscale.

I. INTRODUCTION

THE understanding of the electrical properties of a near-equilibrium bulk conductor can be made clear from the backscattering point of view [1]. The backscattering events in the conductor have been systematically treated, leading to a functional expression for r_c , the well-known backscattering coefficient at the injection point

$$r_c = \frac{L}{L + \lambda_o}. \quad (1)$$

Here, L is the length of the conductor, and λ_o is the equilibrium mean free path for backscattering. Once r_c is known, the total resistance of the conductor can be determined accordingly. Note that, in the case of quasi-ballistic transport (i.e., $\lambda_o > L$), (1) remains valid [1]. Essentially, (1) can apply to the channel backscattering in MOSFETs under near-equilibrium conditions [2]. Extension to the saturation regime of operation can be done by simply replacing the conductor's length L in (1) with the width designated l of a localized *quasi-equilibrium* zone near the source, namely, $k_B T$ layer [2], [3]. The resulting expression reads as [2], [3]

$$r_c = \frac{l}{l + \lambda_o}. \quad (2)$$

Manuscript received July 18, 2008. Current version published November 26, 2008. This work was supported by the National Science Council of Taiwan under Contract NSC 95-2221-E-009-285. The review of this brief was arranged by Editor C. McAndrew.

M. J. Chen and C. Y. Hsu are with the Department of Electronics Engineering, National Chiao Tung University, Hsinchu 300, Taiwan (e-mail: chenmj@faculty.nctu.edu.tw).

L. F. Lu was with the Department of Electronics Engineering, National Chiao Tung University, Hsinchu 300, Taiwan. He is now with the Taiwan Semiconductor Manufacturing Company, Hsinchu 300, Taiwan.

Digital Object Identifier 10.1109/TED.2008.2006532

Within the context of the channel backscattering [2], [3], λ_o is the only mean free path for all operating conditions. More recently, however, sophisticated Monte Carlo simulation studies [4]–[7] have pointed to the significance of the carrier heating in $k_B T$ layer or, in general, the nonequilibrium transport over the channel. In a sense, the carrier heating factor has been incorporated [7] by replacing λ_o in (2) with the *apparent* mean free path λ_1 , thus constituting a new expression

$$r_c = \frac{l}{l + \lambda_1}. \quad (3)$$

In particular, in case of nondegenerate statistics, the Monte Carlo simulations at room temperature on a *linear* channel potential profile have exhibited a certain relationship (see [7, Fig. 4]): $\lambda_1 = \lambda_o/\gamma$ with $\gamma = 1.5$ to 2.0, different at all from that ($\lambda_1 = \lambda_o$) in the literature [2], [3]. Thus, some clarifications are demanded.

To achieve the goal, in this brief, the Monte Carlo particle simulations are performed on a silicon bulk conductor for different conductor lengths, lattice temperatures, and potential profiles. Then, the *apparent* mean free path for backscattering in the $k_B T$ layer is extracted and compared with the equilibrium ones of a long conductor. The results can adequately apply to the channel backscattering in *bulk* nano-MOSFETs. The reasons are that the underlying carrier degeneracy is quite weak, as reflected by an existing low value (= 1.13 for a 1-V gate voltage, as cited in [8, Fig. 4]) of the Fermi–Dirac to Maxwellian injection velocity ratio. In addition, this argument holds as compared with the ultrathin film counterparts, where the carrier degeneracy is pronounced due to the *space confinement effect*. The potential profile under study is not self-consistent but *frozen*, as frequently adopted elsewhere [7], [9], [10], which allows a *direct* examination of the mean-free-path issue.

II. MONTE CARLO SIMULATION

A Monte Carlo particle simulation program dedicated to the solving of the complicated scattering events (i.e., acoustic phonon scattering, optical phonon scattering, and ionized impurity scattering) in a silicon bulk conductor has been developed elsewhere [11]. This program named SDemon (currently merged into a new one called DEMONs [11]) can provide the rich information concerning the carrier positively and negatively directed velocity distributions in the transport direction. The boundary conditions used are as follows: 1) At the origin $x = 0$, the hemi-Maxwellian carriers are injected while, in

the steady state, absorbing the backscattered carriers without further reflections; and 2) at the end of the conductor ($x = L$), the positively directed carriers are absorbed without any ones injected. At the injection point $x = 0$, the ratio of the negatively directed flux to the positively directed flux yields the backscattering coefficient r_c . In the previous work [12] on 80-nm silicon conductor of 10^{12} cm^{-3} doping with a linear potential profile, the simulation program SDemon has been validated in terms of the extracted mobility versus temperature that has been found to be comparable with the published silicon mobility data [13]. The same simulation works are executed here but with the following significant augmentations: a parabolic potential profile added; four different conductor lengths of 15, 25, 50, and 100 nm; and three different lattice temperatures of 150, 200, and 300 K. According to the backscattering framework [2], [3], l can be explicitly expressed as a function of the conductor length L , the thermal energy $k_B T$, and the applied voltage V_a : $l = L k_B T / q V_a$ for the linear potential profile and $L \sqrt{k_B T / q V_a}$ for the parabolic one.

III. RESULTS AND COMPARISONS

On the longest conductor ($L = 100 \text{ nm}$), the outcome of the simulation over $10^{-5} \text{ V} \leq V_a \leq 10^{-3} \text{ V}$ furnishes the quantities of the near-equilibrium r_c . Indeed, the r_c of a linear potential profile is found to be close to that of the parabolic one, as expected. The corresponding λ_o is 56, 105, and 155 nm for 300, 200, and 150 K, respectively. Moreover, the extracted value of λ_o at room temperature is identical to that of the previous work [12].

Unlike its near-equilibrium counterparts, the curvature of the potential profile for $V_a \gg k_B T / q$ can play a relevant role in determining r_c . First of all, in a linear potential profile, the simulated r_c is shown in Fig. 1 for different temperatures versus applied voltage with the conductor length as a parameter. Also shown in the figure are the calculated results from (4) with known λ_o as input [9]

$$r_c = \frac{1 - \exp(-\frac{L}{l})}{1 + \eta \frac{\lambda_o}{l} - \exp(-\frac{L}{l})} \quad (4)$$

where η is the potential profile dependent coefficient and equals unity in the linear potential profile. The primary reasons of using (4) rather than directly (2) are that it can adequately produce r_c in the proximity of zero applied voltage while exactly reducing to (2) for $V_a \gg k_B T / q$ or equivalently $L \gg l$ (see [9] for details). It can be seen that significant deviations are created with respect to the calculation results. In particular, this error increases with increasing applied voltage or decreasing conductor length. It is noteworthy that the lattice temperature does not significantly affect such trends. Indeed, the discrepancies in Fig. 1 can provide the opportunity to examine the mean-free-path issue. By substituting the simulated r_c into the following [9]:

$$r_c = \frac{1 - \exp(-\frac{L}{l})}{1 + \eta \frac{\lambda_1}{l} - \exp(-\frac{L}{l})} \quad (5)$$

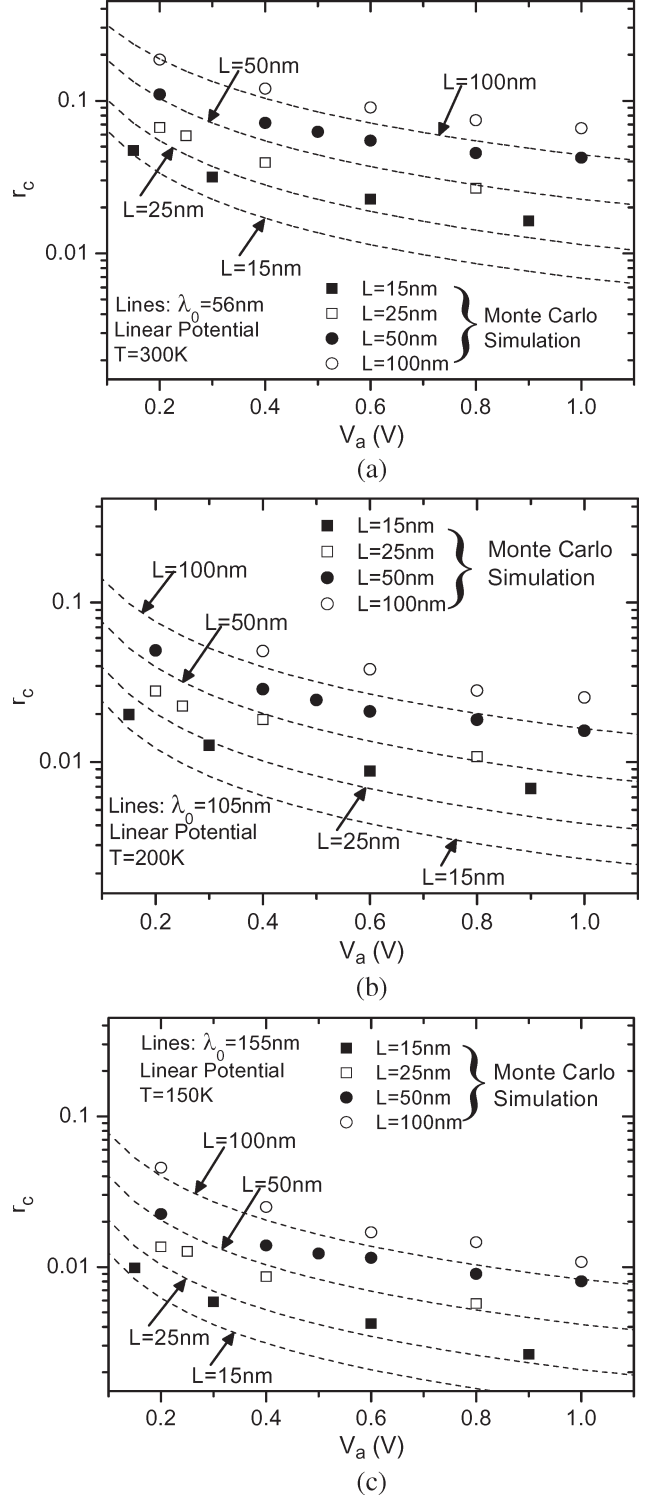
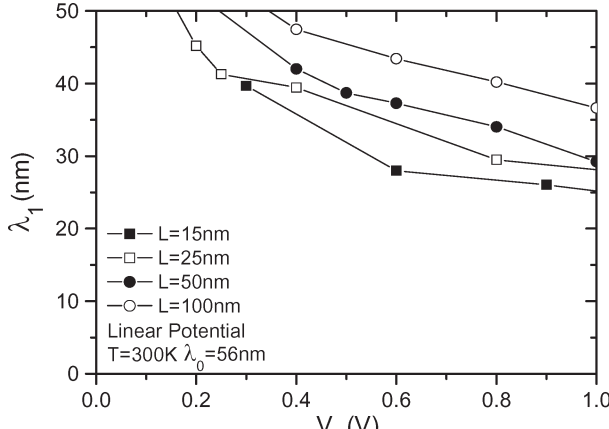
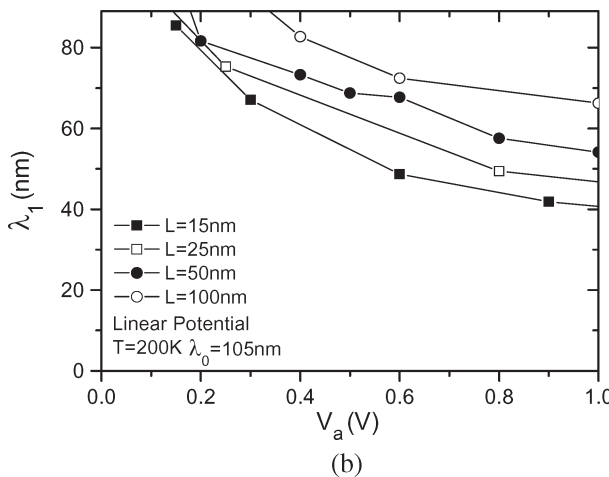


Fig. 1. (Symbols) Simulated r_c in a linear potential profile for four conductor lengths versus applied voltage for (a) 300 K, (b) 200 K, and (c) 150 K. Also shown for comparison are (lines) the calculated results from (4) with $\eta = 1$.

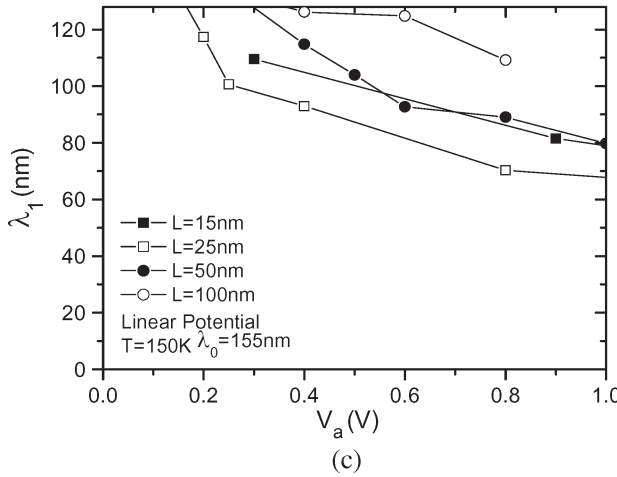
the underlying λ_1 can be extracted, as shown in Fig. 2 versus the applied voltage. It can be seen that 1) λ_1 falls below λ_o ; particularly at 1-V applied voltage, one can draw a specific relation of $\lambda_1 = \lambda_o / \gamma$ with $\gamma = 1.5$ to 2.5; 2) on average, λ_1 decreases with decreasing conductor length; and 3) again on average, λ_1 decreases with the applied voltage. It is therefore



(a)



(b)

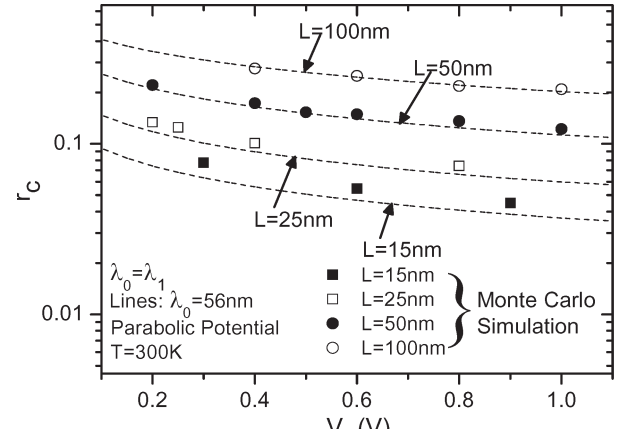


(c)

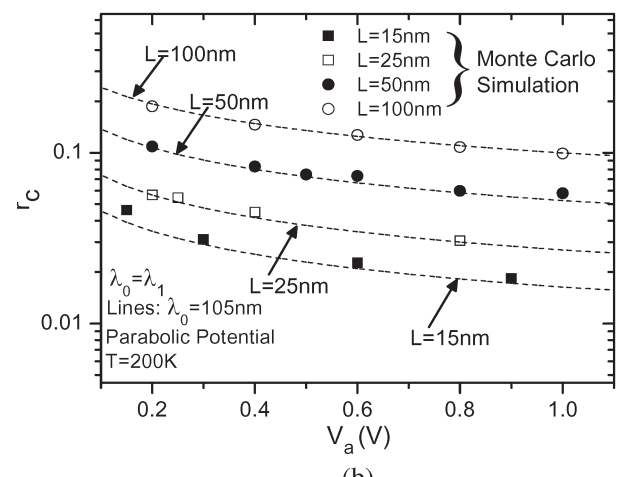
Fig. 2. Extracted *apparent* mean free path λ_1 via (5) with $\eta = 1$ corresponding to the data points in Fig. 1 for (a) 300 K, (b) 200 K, and (c) 150 K.

inferred that only with increasing conductor length or decreasing applied voltage can the upper limit of λ_o be recovered. Once again, the ratio of λ_1 to λ_o appears to be a weak function of the lattice temperature. Note that the recent Monte Carlo simulations [7], devoted to a linear potential profile at 300 K, have produced similar results, as mentioned earlier.

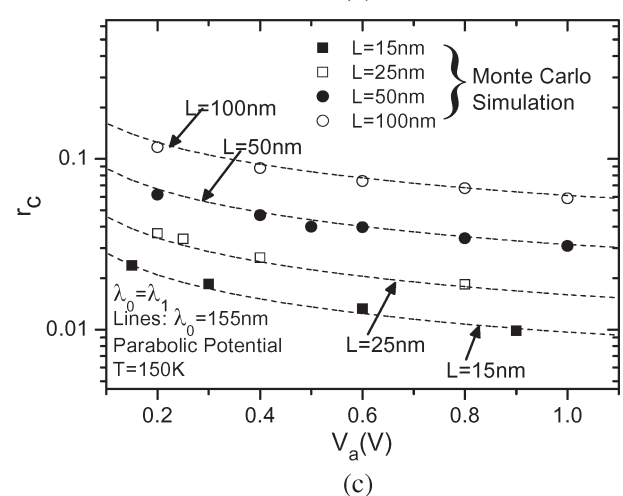
For the parabolic potential profile, the corresponding simulation results are shown in Fig. 3. Also shown are the calculated lines from (5) with $\eta = 2/\sqrt{\pi}$ (see [9, Eq. (37)]) and $\lambda_1 = \lambda_o$,



(a)



(b)



(c)

Fig. 3. Comparison of the (symbols) simulated and (lines) calculated r_c 's for four conductor lengths in a parabolic potential profile versus applied voltage for (a) 300 K, (b) 200 K, and (c) 150 K. The calculations are from (5) with $\eta = 2/\sqrt{\pi}$ [9] and $\lambda_1 = \lambda_o$.

105, and 155 nm for 300, 200, and 150 K, respectively. We found that good reproduction of data points for different conductor lengths, temperatures, and applied voltages can all be achieved with simply $\lambda_1 = \lambda_o$, without adjusting any parameters. This means that, despite the quasi-ballistic transport prevailing in the $k_B T$ layer ($\lambda_1 > l$), the quasi-equilibrium conditions still govern the backscattered carriers.

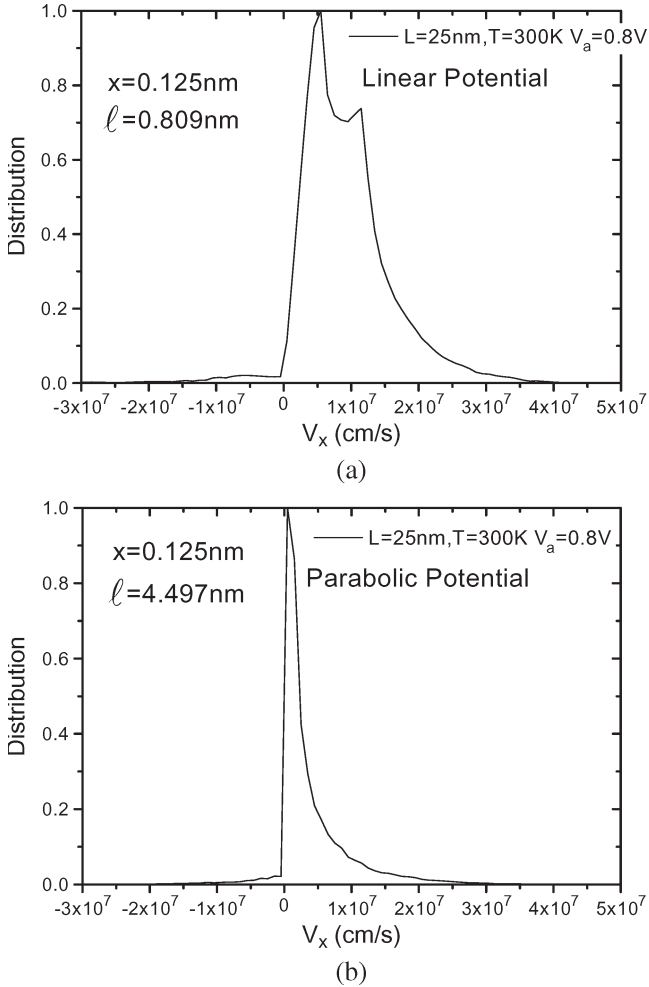


Fig. 4. Simulated carrier velocity component distribution in the transport direction at $x = 0.125$ nm for (a) a linear potential profile and (b) a parabolic potential profile. $L = 25$ nm, $T = 300$ K, and $V_a = 0.8$ V.

IV. EVIDENCE FOR CARRIER HEATING

Here, we demonstrate that the different mean free paths between the parabolic and linear potential profiles can be traced to the curvature of the potential profile, particularly the presence or absence of a zero or weak field regime near the injection point. For a parabolic potential profile, there is a significant fraction of the $k_B T$ layer, which can be identified as the zero-field regime. With this in mind, although the deviations from the lattice temperature would be possible as entering into the remainder (i.e., out of the zero-field regime), the overall carrier heating in the $k_B T$ layer should be weakened. For a linear potential profile, however, such a zero-field regime is lacking. Therefore, once injected at the beginning of the $k_B T$ layer, the carriers immediately undergo acceleration from the nonzero field. Owing to the quasi-ballistic transport (less collision), the carrier temperature is expected to be higher than the lattice temperature, and the mean free path is therefore no longer independent of the carrier energy. The confirmative evidence is presented in terms of the carrier velocity component v_x distribution in the transport direction near the injection point, as shown in Figs. 4 and 5 for $L = 25$ nm at $V_a = 0.8$ V and 300 K and $L = 50$ nm at $V_a = 1.0$ V and 150 K, respectively.

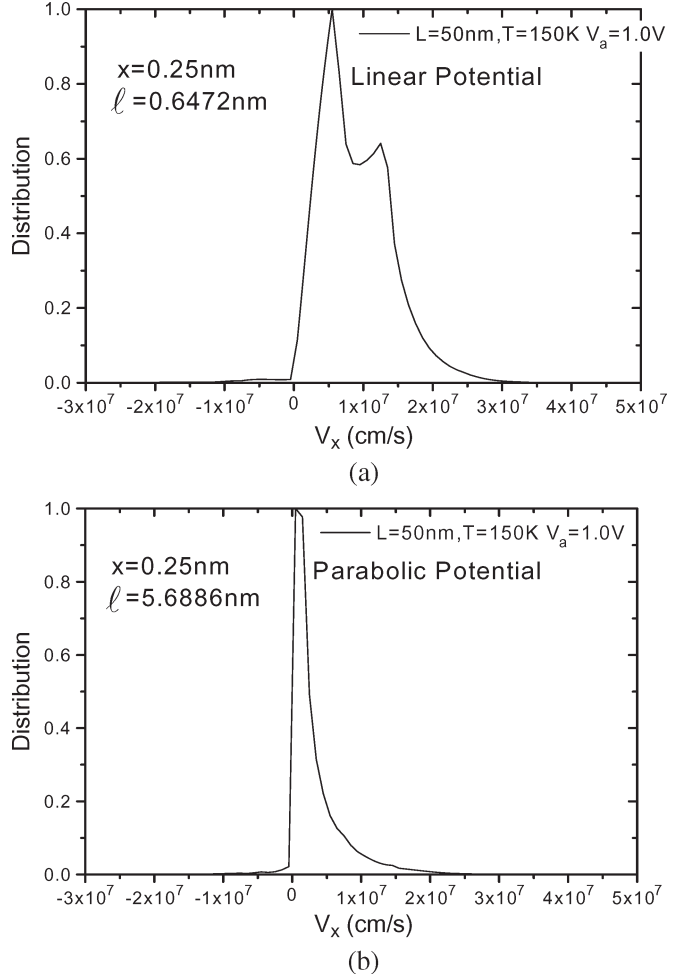


Fig. 5. Simulated carrier velocity component distribution in the transport direction at $x = 0.25$ nm for (a) a linear potential profile and (b) a parabolic potential profile. $L = 50$ nm, $T = 150$ K, and $V_a = 1.0$ V.

They are all created by the program DEMONs. These figures clearly reveal two significant differences between the potential profiles. First, in a parabolic potential profile, a single hemi-Maxwellian distribution is retained in the positively directed carriers but is split into two distinct components in the linear potential case: One of the longitudinal effective masses and one of the transverse effective masses. This strongly points to the effect of the nonzero field in the linear potential profile. Second, the distribution of the negatively directed or backscattered carriers appears to be wider in a linear potential profile than the parabolic one.

V. CONCLUSION

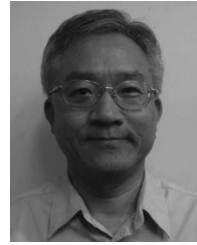
The Monte Carlo simulations have been extensively carried out on a silicon bulk conductor aimed at reexamining the channel backscattering in bulk nano-MOSFETs. The main results achieved in this brief can be summarized as follows.

- 1) The near-equilibrium mean free path for backscattering λ_o is independent of the potential profile.
- 2) The apparent mean free path λ_1 in a localized quasi-ballistic $k_B T$ layer can be linked with the curvature of the potential profile.

- 3) The λ_1 in a linear potential profile is lower than λ_o due to the presence of the carrier heating, as highlighted by the carrier velocity distribution near the injection point.
- 4) In a parabolic potential profile, the mean free paths remain consistent: $\lambda_1 = \lambda_o$. This means that, despite the quasi-ballistic transport prevailing in the $k_B T$ layer ($\lambda_1 > l$), the quasi-equilibrium conditions still govern the backscattered carriers.

REFERENCES

- [1] S. Datta, *Electronic Transport in Mesoscopic Systems*. Cambridge, U.K.: Cambridge Univ. Press, 1995, ch. 2, pp. 62–65.
- [2] M. S. Lundstrom, “Elementary scattering theory of the Si MOSFET,” *IEEE Electron Device Lett.*, vol. 18, no. 7, pp. 361–363, Jul. 1997.
- [3] M. S. Lundstrom and Z. Ren, “Essential physics of carrier transport in nanoscale MOSFETs,” *IEEE Trans. Electron Devices*, vol. 49, no. 1, pp. 133–141, Jan. 2002.
- [4] C. Jungemann, N. Subba, J. S. Goo, C. Riccobene, Q. Xiang, and B. Meinerzhagen, “Investigation of strained Si/SiGe devices by MC simulation,” *Solid State Electron.*, vol. 48, no. 8, pp. 1417–1422, Apr. 2004.
- [5] J. Saint Martin, A. Bournel, and P. Dollfus, “On the ballistic transport in nanometer-scaled DG MOSFETs,” *IEEE Trans. Electron Devices*, vol. 51, no. 7, pp. 1148–1155, Jul. 2004.
- [6] P. Palestri, D. Esseni, S. Eminente, C. Fiegn, E. Sangiorgi, and L. Selmi, “Understanding quasi-ballistic transport in nano-MOSFETs: Part I—Scattering in the channel and in the drain,” *IEEE Trans. Electron Devices*, vol. 52, no. 12, pp. 2727–2735, Dec. 2005.
- [7] P. Palestri, R. Clerc, D. Esseni, L. Lucci, and L. Selmi, “Multi-subband-Monte-Carlo investigation of the mean free path and of the kT layer in degenerated quasi ballistic nanoMOSFETs,” in *IEDM Tech. Dig.*, Dec. 2006, pp. 945–948.
- [8] M. J. Chen, H. T. Huang, Y. C. Chou, R. T. Chen, Y. T. Tseng, P. N. Chen, and C. H. Diaz, “Separation of channel backscattering coefficients in nanoscale MOSFETs,” *IEEE Trans. Electron Devices*, vol. 51, no. 9, pp. 1409–1415, Sep. 2004.
- [9] R. Clerc, P. Palestri, and L. Selmi, “On the physical understanding of the kT -layer concept in quasi-ballistic regime of transport in nanoscale devices,” *IEEE Trans. Electron Devices*, vol. 53, no. 7, pp. 1634–1640, Jul. 2006.
- [10] M. J. Chen and L. F. Lu, “A parabolic potential barrier-oriented compact model for the $k_B T$ layer’s width in nano-MOSFETs,” *IEEE Trans. Electron Devices*, vol. 55, no. 5, pp. 1265–1268, May 2008.
- [11] [Online]. Available: <https://www.nanohub.org>
- [12] M. J. Chen, S. G. Yan, R. T. Chen, C. Y. Hsieh, P. W. Huang, and H. P. Chen, “Temperature-oriented experiment and simulation as corroborating evidence of MOSFET backscattering theory,” *IEEE Electron Device Lett.*, vol. 28, no. 2, pp. 177–179, Feb. 2007.
- [13] C. Jacoboni, C. Canali, G. Ottaviani, and A. A. Quaranta, “A review of some charge transport properties of silicon,” *Solid State Electron.*, vol. 20, no. 2, pp. 77–89, Feb. 1977.



Ming-Jer Chen (S’78–M’79–SM’98) received the B.S. degree in electrical engineering (with highest honors) from the National Cheng Kung University, Tainan, Taiwan, in 1977 and the M.S. and Ph.D. degrees in electronics engineering from the National Chiao Tung University (NCTU), Hsinchu, Taiwan, in 1979 and 1985, respectively.

Since 1985, he has been with the Department of Electronics Engineering, NCTU. He has become a Full Professor since 1993. From 1987 to 1992, he was a Consultant with the Taiwan Semiconductor

Manufacturing Company, where he led a team from the NCTU and the Electronics Research and Service Organization/Industrial Technology Research Institute to build up a series of process windows and design rules. From 2000 to 2001, he was a Visiting Professor with the Department of Electrical Engineering and the Center for Integrated Systems, Stanford University, Stanford, CA. He is the holder of eight U.S. patents and six Taiwanese patents in the field of the high-precision analog capacitors, 1-T memory cell, dynamic threshold MOS, electrostatic discharge protection, and Flash memory. He has graduated 14 Ph.D. students and more than 100 M.S. students. His current research interests include semiconductor device physics and nanoelectronics.

Dr. Chen is a member of the Phi Tau Phi.



Li-Fang Lu was born in Taoyuan, Taiwan, in 1982. He received the B.S. degree in electrophysics and the M.S. degree in electronics engineering from the National Chiao Tung University, Hsinchu, Taiwan, in 2006 and 2008, respectively.

He is currently with the 32-nm/40-nm Technology R&D Department, Taiwan Semiconductor Manufacturing Company, Hsinchu, as a 300-mm Wafer Process Integration Engineer. His main research interest is on the physics of the backscattering phenomenon in nanoscale devices.



Chih-Yu Hsu (S’07) received the B.S. degree in electrophysics from the National Chiao Tung University, Hsinchu, Taiwan, in 2005, where he is currently working toward the Ph.D. degree in electronics engineering in the Department of Electronics Engineering.

His research interests include the characterization and modeling of the strained-Si MOSFETs and the trap physics in nanoscale devices.